ResearchGate

See discussions, stats, and author profiles for this publication at: https://www.researchgate.net/publication/231642521

Self-Assembled Monolayers of β-Alkylated Oligothiophenes on Graphite Substrate: Molecular Dynamics Simulation

ARTICLE *in* THE JOURNAL OF PHYSICAL CHEMISTRY C · APRIL 2007

Impact Factor: 4.77 · DOI: 10.1021/jp0704618

CITATIONS
18

READS
4

6 AUTHORS, INCLUDING:

Elena Mena-Osteritz
Universität Ulm
58 PUBLICATIONS **1,924** CITATIONS
SEE PROFILE

Pavel G. Khalatur
Universität Ulm
235 PUBLICATIONS **2,495** CITATIONS
SEE PROFILE

Peter Bäuerle
Universität Ulm
356 PUBLICATIONS **13,152** CITATIONS
SEE PROFILE

Available from: Pavel G. Khalatur
Retrieved on: 25 January 2016

Self-Assembled Monolayers of β-Alkylated Oligothiophenes on Graphite Substrate: Molecular Dynamics Simulation

Olga A. Gus'kova,[†,‡] Elena Mena-Osteritz,[§] Eva Schillinger,[§] Pavel G. Khalatur,*[,†,‡] Peter Bäuerle,[§] and Alexei R. Khokhlov[‡,||]

Department of Physical Chemistry, Tver State University, Tver 170002, Russia, Department of Polymer Science and Department of Organic Chemistry II, University of Ulm, Ulm D-89069, Germany, and Physics Department, Moscow State University, Moscow 119899, Russia

Received: January 19, 2007; In Final Form: March 17, 2007

Atomistic molecular dynamics simulations have been used, apparently for the first time, to investigate self-assembly and organization of β-alkylated oligothiophenes adsorbed on graphite. We demonstrate that side-chain substitution is an effective means for the modification of molecular conformation and surface morphology. Comparisons between the unsubstituted tetrathiopene (4T) deposited on graphite and the β-alkylated oligothiophenes demonstrate that the presence of long hydrocarbon side chains in 4T produces monolayer films with a higher degree of order at the molecular level. The results are in qualitative agreement with experiments.

Introduction

Semiconducting conjugated polymers and oligomers are of considerable interest as active organic materials in electronic and optoelectronic devices such as light-emitting diodes (LEDs) for display applications, polymer lasers, photovoltaic cells, and field-effect transistors (FETs) for use in plastic smart chips.[1−5] A wide range of conjugated polymer systems has been synthesized, including poly(*p*-phenylene), poly(1,4-phenylenevinylene), polyfluorene, polythiophenes, and their derivatives (see, e.g., refs 2, 3, and 5). One of the most promising conjugated (macro)molecules for various nanoelectronic applications are those based on oligo- and polythiophenes because of their good thermal and chemical stability, low electronic $\pi \rightarrow \pi^*$ band gaps, as well as their optical properties, such as, for example, enhanced luminosity and very pure colors. It is not surprising that these compounds have become the subject of great interest over recent years.

The functions of conjugated polymer-based devices are determined by their nanostructure, which depends on interpolymer packing and conformation of conjugated polymers in the solid state. The intramolecular and intermolecular effects also strongly affect photophysical and charge transport properties of the materials. However, the development of effective and precise methods for controlling the nanostructure of conjugated polymers in the solid state is limited because those polymers often fail to assemble into organized structures due to their low solubility, large molecular weight, polydispersity, and amorphous character.

Organic thin film transistors, LEDs, and photovoltaic cells typically consist of one or more layers, which can be obtained by different techniques, including spin coating, casting vapor deposition, etc. One of the possible approaches in creating self-organized organic monolayers is the formation of those layers by adsorption from a solution onto a solid substrate. Unfortunately, for polythiophenes, these methods often produce amorphous or semicrystalline materials with little control over the positional and conformational order. Oligothiophenes, which themselves represent excellent candidates for electronic materials and inorganic−organic hybrid devices, generally offer better processability. Because π-conjugated oligothiophenes possess good solubility and can be sublimated, the control over their supramolecular organization on the nanoscale can be achieved via the formation of ultrathin films on surfaces using surface modification techniques such as molecular vapor deposition and traditional solution or other vapor deposited coatings. Moreover, it is easy to modify their main characteristics by attaching different functional groups, either to the β-positions of the rings or to the two terminal α-positions, and by controlling their regioregularity.[4,5] Indeed, in a series of publications,[6−19] it has been demonstrated that different chemically modified oligothiophenes can form highly ordered monolayers at the solid−liquid and solid−air interfaces.

In particular, Fukunaga et al.[9] observed the two-dimensional organization at the liquid−graphite interface of monothiophene functionalized in the β-position with a long alkyl chain. In this study, the thiophene molecules were found to be lying head-to-head, with the five-membered rings oriented diagonally on the graphite surface and stacked face-to-face. Bäuerle et al. used scanning tunneling microscopy (STM) to study β-alkylated oligothiophenes with long alkyl side chains at the highly oriented pyrolitic graphite (HOPG).[10−12] They observed the formation of ordered two-dimensional (2-D) textures that depend on the length of the oligothiophene section and hydrocarbon chain. The 2-D arrangement of a series of alkylated sexithiophenes has also been investigated at the liquid−graphite interface.[13] The influence of an increasing polarity of the substituents on the 2-D texture of oligothiophenes physisorbed on graphite has been investigated by Stecher et al.[14,15] Azumi et al. described the results of an analysis and comparison of the molecular conformation and packing of the very long, fully α-conjugated and

* To whom correspondence should be addressed. E-mail: khalatur@germany.ru.
[†] Tver State University.
[‡] Department of Polymer Science, University of Ulm.
[§] Department of Organic Chemistry II, University of Ulm.
[||] Moscow State University.

10.1021/jp0704618 CCC: $37.00 © 2007 American Chemical Society
Published on Web 04/25/2007

structurally defined alkylated dodecilthiophene (12T) both in a single crystal and in a 2-D self-assembled monolayer adsorbed at the liquid−solid interface.[16,17] To control the ordering of molecules in the 2-D monolayer structure, directional noncovalent modes of interaction, such as hydrogen bonding, are of great help and importance. In addition to their directional properties, they may control intermolecular distances and as a result dictate the molecular conformation and properties. Gesquière et al. reported on a structural investigation of the 2-D supramolecular organization of three bis-urea-substituted thiophene derivatives, containing one, two, or three thiophene units, at the solution−graphite interface with STM.[18] It was found that hydrogen bonding between the urea groups of adjacent molecules controls the spatial arrangement on the graphite surface.[18,19]

Although many experimental studies have been performed on the adsorption of oligothiophene and its derivatives on different substrates, the control over supramolecular self-assembly or the formation of a particular polymorph is still limited and rather primitive. On the theoretical side, it is known that without an external periodic field in a 2-D system, there can be no long-range pair positional order (that is, no δ-function Bragg peaks), so the 2-D crystalline solid is qualitatively different from the 3-D one.[20,21] The fundamental effect of the introduction of a surface into a system capable of ordering is to break its translational symmetry. In addition to breaking the translational symmetry, the surface selects a subset of the degenerate orientational states. In the absence of competing forces such as those that might be generated by an external electric field, the orientation selected by the interaction with the surface propagates into the bulk as a result of intermolecular interactions. Therefore, understanding the effects of a periodic field caused by a substrate on the 2-D texture formed at the physisorption of molecules is clearly one of the central issues here. Another important problem is related to understanding the influence of substituents on the 2-D organization of thiophene derivatives. This area is addressed in the present theoretical study, which is based on atomistic molecular dynamics (MD) simulations. The long-term goal of this research is to examine, through molecular modeling, the impact of multiple chain (or aggregation) effects on electro-optical and structural properties of polythiophene-based materials, including those functionalized with oligopeptide sequences. Computational methods and atomistic modeling have a great potential to optimize the synthesis condition and structures of these complex compounds.

In this work, we focus on the static properties of physisorbed $-\beta$-alkylated oligothiophenes. We model the adsorption process together with the early organization of the thiophene oligomers at the graphite surface. The inter- and intra-atomic forces acting between atoms in the thiophene subsystem are calculated using the OPLS/AA-like force field, whereas the graphite surface is included as an additional stationary external potential, based on pairwise Lennard-Jones (LJ) interactions between the atoms in the graphite surface and the atoms in the thiophene subsystem.

There are several simulation studies of physisorbed oligothiophenes. Gesquière et al. performed a short MD simulation of bis-urea-substituted thiophene derivatives functionalized in the α-position at the solution−graphite interface.[18] It was shown that the thiophene rings are tilted with respect to the surface and have partially overlapping π-systems. Marcon et al. carried out MD simulations of α-tetrathiophene molecules deposited on a flat graphite substrate.[22] For the systems at different degrees of surface coverage, they found that the molecules in the first adsorption layer are relatively planar and are packed against the underlying surface, while those outside the first layer are not arranged in well-defined layers and are more conformationally disordered. It was shown that on the time scale of the simulation (5 ns), the oligomers did not crystallize but formed a liquid crystalline-like state with their average director parallel to the surface. The deposition of tetrathiophene molecules on the (010) surface of potassium hydrogen phthalate was also simulated.[23] A grand canonical ensemble Monte Carlo simulation was performed to investigate the adsorption, heat of adsorption, and distributions of thiophene in all-silica Y and Na−Y zeolites.[24] Recently, Surin et al. have reported on a joint experimental and theoretical approach for the study of the assembly of end-substituted (α-substituted) oligothiophenes at surfaces with different polarities (mica vs graphite).[25] Using molecular modeling with an atomistic approach, they focused on the interplay between the molecule−molecule (and segment−segment) interactions and the molecule−substrate interactions and their influence on the observed morphologies and the stacking geometry.

SCHEME 1

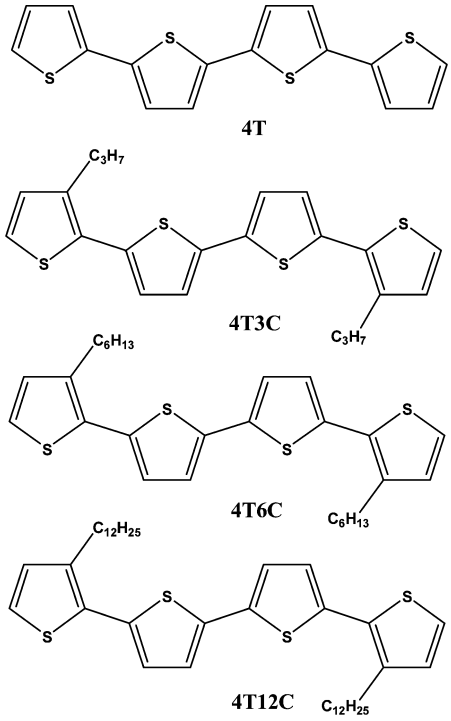

Computational Model and Methods

Molecular Model of Oligothiophenes. The following three compounds were studied: 3,3‴-dipropyl-quaterthiophene (4T3C), 3,3‴-dihexyl-quaterthiophene (4T6C), and 3,3‴-didodecyl-quaterthiophene (4T12C); see Scheme 1. As a reference system, we considered α-tetrathiophene (4T).

The structural parameters and partial charges of the β-alkylated oligothiophenes were found using ab initio calculations at the HF/6-31G*//MP2/6-31G+* level. The minimum energy structures were first determined at the semiempirical AM1 level. The resulting structures were then used as an input for subsequent optimization at the HF level. Fully optimized molecular geometries were found using the Polak−Ribiere conjugate gradient method. The minimizations were terminated when the total energy of the potential energy hypersurface reached an rms force gradient of <0.01 kcal/mol/Å. Finally, the optimized geometries were used for single point MP2 calculations that also gave the partial charges on atoms.

There are two kinds of interactions involved in the simulation of adsorption layers, namely, adsorbate−adsorbate and adsorbent−adsorbate interactions. In our MD simulations, we employed the OPLS/AA-like force field[26−28] supplemented by some additional parameters related to the rotation of thiophene rings and the adsorbent−adsorbate interactions. The recent simulation of the growth of tetrathiophene (4T) films from the vapor phase has shown[23] that this force field is both simpler and more satisfactory than previous ones, which adopted, for example, the MM3 parameters[29] (see also ref 30).

The total potential energy of the system was represented as a sum of the bond stretching, bond angle bending, and dihedral torsion energies as well as the van der Waals (LJ) and electrostatic (Coulomb) terms, $V = V_b + V_\Theta + V_\varphi + V_{vdw} + V_e + V_{surf}$. Here, the last term describes the external static potential due to the surface acting on the adsorbate atoms. Both short-range van der Waals and long-range electrostatic interactions between all atoms were explicitly included in the model. LJ parameters for the cross interactions were obtained using the Lorentz−Berthelot combining rules.

Ab initio methods applied to unsubstituted bithiophene (2T) show that two five-membered rings are not planar and that two conformers can coexist in the gas phase or in solution. These two conformations correspond to the S−C−C−S dihedral angle of about 150° (global minimum) and about 30° (local minimum). The twisted conformations observed for 2T are due to an interplay between two opposite forces: the electron delocalization along the molecular axis that favors a planar geometry and the strong steric repulsion between hydrogen atoms in positions 3 or 3′ and the sulfur atoms (for the anti conformation) or between the two sulfur atoms and the two hydrogen atoms in positions 3 and 3′ (for the syn conformation).[31−33] The intrinsic torsion potentials of dihedral angles were defined in the MM3 fashion[22,31−33] as follows:

$$V_\varphi = \sum_{\text{bonds}} \sum_i v_i[1 - \cos(i\varphi - \varphi_0)] \qquad (1)$$

where v_i and φ_0 are the torsional parameters. Note that the generic OPLS/AA force field gives the most stable structure where the thiophene rings are antiplanar (S−C−C−S torsion angle of 180°), which is adequate to simulate the solid-state behavior of conjugated compounds or their strongly adsorbed state.

Because we simulated an open system without periodic boundary conditions, the electrostatic interactions in the simulations were computed using the generalized reaction field (GRF) method based on the linearized Poisson−Boltzmann (PB) approach.[34] In this method, each charged atom is treated as the origin of a spherical coordinate system. The charge is surrounded by a cutoff sphere containing explicit neighboring charges, itself placed within a homogeneous dielectric continuum of permittivity equal to that of the solvent and of specified ionic strength. To estimate the reaction field force from the continuum onto the atom, the PB equations of continuum electrostatics were solved using spherical symmetry, assuming a uniform continuum of given ionic strength beyond the cutoff distance. As a result, a particular solution for the electrostatic potential and its derivative at the center of the sphere was obtained. In this study, the relative dielectric constant ϵ was chosen to be 1, but the choice is not very critical. Indeed, experimentally, no significant polarity effect on the solution properties of substituted oligothiophenes, including their molecular photophysics, was observed.[35] For the calculation, we used the standard point-charge model that is known to yield satisfactory results for a series of substituted thiophene oligomers in the solid state.[29] In particular, it has been found that the densities and the heats of sublimation are almost unaffected by the choice of the electrostatic model.[29]

Graphite. The highly oriented pyrolitic graphite (HOPG) was treated in full atomic detail. We first built a single (001) surface plane (of 47 × 47 six-membered fused rings, 4608 carbon atoms) using appropriate lattice parameters[36] ($a = b = 2.46$ Å, $c = 6.80$ Å, $\alpha = \beta = 90°$, and $\gamma = 120°$) and saturating with hydrogen atoms the dangling bonds at the edges. For the graphite surface, these geometric parameters match a real graphite structure with nearest neighbor carbon atoms separated by 1.42 Å. Since the graphite atoms do not possess partial charges, the interactions between the adsorbed molecules and the surface are simply of van der Waals type. Therefore, the V_{surf} term describing the adsorbent−adsorbate interactions was written based on pairwise LJ interactions and on the translational symmetry of the substrate.[37,38] The graphite substrate was rigid throughout the simulation, making the specification of surface−surface interactions unnecessary. In other words, the carbon atoms of the graphite were kept fixed in their equilibrium position since physisorption is not expected to alter the geometry of the substrate surface.

Initial Configurations and Their Relaxation. To obtain a many-molecule system, n identical molecules ($n = 42$ for 4T, $n = 30$ for 4T3C, $n = 45$ for 4T6C, and $n = 30$ for 4T12C; the corresponding surface coverage is 0.111, 0.127, 0.262, and 0.270 atoms/Å^2) having a fully optimized geometry were initially placed on a regular lattice with the conjugated plane parallel to the surface of the substrate, typically 4 Å from the surface plane, and then were randomly reoriented. To remove the overlaps between atoms brought about by the omission of the intermolecular interactions during the initial generation procedure, a short MD run was performed with the bending, torsion, and electrostatic interactions switched on, while the LJ potential was introduced very gradually. At this initial stage, velocities were rescaled at each time step to compensate for the large amount of heat produced in the system.

MD Simulation. The systems were simulated at a constant number of atoms and constant temperature, $T = 300$ K. Also, two additional runs were carried out at 200 and 100 K. The temperature was maintained by the Nose−Hoover thermostat[39,40] using the modular-invariant method.[41] The corresponding Nose NVT relaxation time, τ_T, was set to 30 fs. The equations of motion were integrated using the reversible double time step algorithm[42] in which all the forces are divided into two groups, fast and slow. The first one is due to covalent bonds, bond angles, and dihedral angles; it also includes LJ forces and electrostatic forces within a short cutoff distance, R_s, of 5 Å. The second group includes long-range LJ and electrostatic forces on distances between R_s and a long cutoff distance R_c. The truncation radius for LJ and electrostatic interactions was set to $R_c = 15$ Å, and long-range corrections to the energy were made on the assumption that all the pair correlation functions $g(r) = 1$ beyond the cutoff.[43] The equations of motion were solved using a leapfrog version of the Verlet−Störmer algorithm[44] with a fast time step, Δt_f, of 0.3 fs and a slow time step $\Delta t_s = 10\Delta t_f$.

Equilibration runs were continued until such properties as potential energy, orientational order parameter, etc. were more or less stabilized. The total length of the equilibration runs was usually 200 ps. In these simulation runs, the total and potential energies showed an initial decrease, possibly with a few separate kinetic stages, and then fluctuated around a constant value, indicating the achievement of the equilibrium state. This process

corresponds to the adsorption and diffusion dynamics of the molecules from the initial configuration. Another measure of the equilibration of the system is the extent to which the molecules are capable of utilizing translational motions, along preferable directions on the graphite surface, in optimizing the packing in the system. That is, it is to be hoped that the translational registration between molecules along these directions should be established by the accessibility of configuration space in the simulation and not imposed by the initial configuration of the system. This point was investigated by sampling the translational positions of the molecules. Configurations and thermodynamic and conformational data were then stored and analyzed over production runs ranging from 3 to 25 ns. Substantial molecular displacements over the sampling interval, on the order of several angstroms at 300 K, were observed. This would appear to be sufficient to indicate participation of this degree of freedom in finding favorable local packing. Within these runs, the total and potential energy fluctuated around a constant value, indicating that an equilibrium state was eventually reached. Different properties were obtained by averaging over the production runs using configurations saved every 1 ps.

For the calculations, we used a Linux cluster system of 32 CPUs and homemade software (for more detail, see refs 45 and 46).

Results and Discussion

We found that generally the molecules adsorb flat against the surface (i.e., the long molecular axis is oriented parallel to the graphite plane). The adsorbed molecules strongly favor stretched conformations. Furthermore, we observed an indication for the onset of clustering and orientational ordering of the adsorbed thiophene oligomers, that is, the molecules exhibit liquid crystalline behavior. Adsorption forces keep the thiophene segments almost planar, despite the torsion potential that tends to favor distorted conformations. Alkyl chains also tend to lie nearly flat on graphite; the presence of long side chains must therefore also favor the flat molecular conformation. Those features are seen well from typical snapshot pictures of equilibrated configurations (Figure 1). The simulation results are, thus, consistent with the previously mentioned experimental findings obtained on similar systems in the regime of a high oligomer surface concentration. Next, we discuss these results in more detail.

It should be noted that for a given geometry of the aromatic backbone, the aliphatic side chains in poly- or oligothiophenes do not have a direct effect on the electronic structure of the π-system of the thiophene rings.[47] However, when the aliphatic chains induce a change in the geometry of the aromatic backbone (as discussed next), then they do affect the electronic structure of the π-system.

Adsorption Layer. We begin with the discussion of the general structural features of the adsorption layer derived from MD simulations. Figure 2a presents the number−density distribution, $\phi(z)$, which characterizes the sample-average number of atoms at the distance z from the graphite surface. All the $\phi(z)$ functions calculated for the four compounds under consideration have a sharp peak at $z \approx 4$ Å that can be associated with the thickness of the adsorption layer. The position of the peak coincides with that found by Marcon et al. for adsorbed 4T.[22] For the substituted oligothiophenes, there are almost no qualitative differences between the density profiles; at $z > 4$ Å, the monotomic decrease of the number−density distribution away from the interface is observed. The thickness of the adsorbed layer is mainly determined by the extension of hydrocarbon tails into the bulk. Indeed, the $\phi(z)$ function demonstrates the steepest decay for 4T3C with short side chains, while for 4T6C and 4T12C, it decays significantly more slowly. For the unsubstituted tetrathiophene system, we observe a second (very weak) peak at $z \approx 7.4$ Å. With the $\pi-\pi$-stacking distance of the thiophene derivatives being estimated to be ≈3.8 Å,[48] and taking into consideration the van der Waals radii, this peak indicates the formation of the second adsorption layer, which is much more diffusive as compared to the first one. As seen from Figure 2a, the density of atoms approaches zero at $z > 10$ Å.

To analyze the separate contribution of the thiophene backbone and of the side chains to the total distribution $\phi(z)$ of the alkyl-substituted oligothiophenes, we additionally calculated two functions $\phi_T(z)$ and $\phi_C(z)$, which characterize the distribution of atoms belonging to the thiophene and alkyl fragments, respectively. These functions are shown in Figure 2a,b. In general, from Figure 2b, we observe that the density profiles $\phi_T(z)$ become sharper as the side-chain length increases. This indicates that the sufficiently long side chains attached to the conjugated backbone induce planarity in the adsorbed backbone as compared to the solution phase in which the backbone is twisted out of coplanarity. The extent of the profiles for 4T6C and 4T12C, however, seems rather insensitive to the side-chain length, although one could intuitively expect a contraction of the profiles as the average adsorption energy per substituted thiophene ring is increased. As seen from Figure 2c, the increase of the side-chain length leads to a considerable broadening of the region occupied by the longer chains and causes the outer part of the adsorption layer to have more room for the long chains. Therefore, we can conclude that the broadening of the peak observed in Figure 2a is mainly due to the contribution of the alkyl tails. These results show that the side chains attached to the backbone of the conjugated oligomers can play a key role in the packing of these conjugated molecules in adsorption layers.

Molecular Organization Near Surface. In the most stable structures on graphite that can be observed in STM images, the thiophene-based oligomers tend to accommodate within the conjugated plane lying parallel to the substrate at an equilibrium distance of 3.5−3.6 Å. This distance is typical for $\pi-\pi$-stacking systems.[49] To characterize the orientation of individual molecules and their fragments in the adsorbed state, we calculated the pseudo-dihedral angle between the thiophene ring and the graphite plane, ω_r, as well as the angle between the graphite plane and the vector connecting the two terminal carbon atoms of the alkyl chain, ω_c.

Figure 3 shows the distribution functions $W(\omega_r)$ and $W(\omega_c)$ obtained by independent averaging over all rings/chains belonging to a given molecule and over all molecules. We found that the $W(\omega_r)$ function has a peak in the vicinity of ±10° for all the compounds under study (Figure 3a illustrates the results for the systems 4T, 4T3C, and 4T12C). This means that the thiophene rings in the adsorbed state can deviate from a perfect planar orientation with respect to the substrate. The deviation increases with decreasing the side-chain length, and for unsubstituted tetrathiophene, there is a maximum of $W(\omega_r)$ at $\omega_r = 90°$, thus indicating that a substantial fraction of the molecules has a perpendicular orientation of the rings. Because the molecules orient with their long axis parallel to the graphite sheet, neither perfect π-stack structures nor herringbone-type assembly[50] (in which the conjugated planes of nearest neighbor molecules are in front of each other) are formed. This geometry

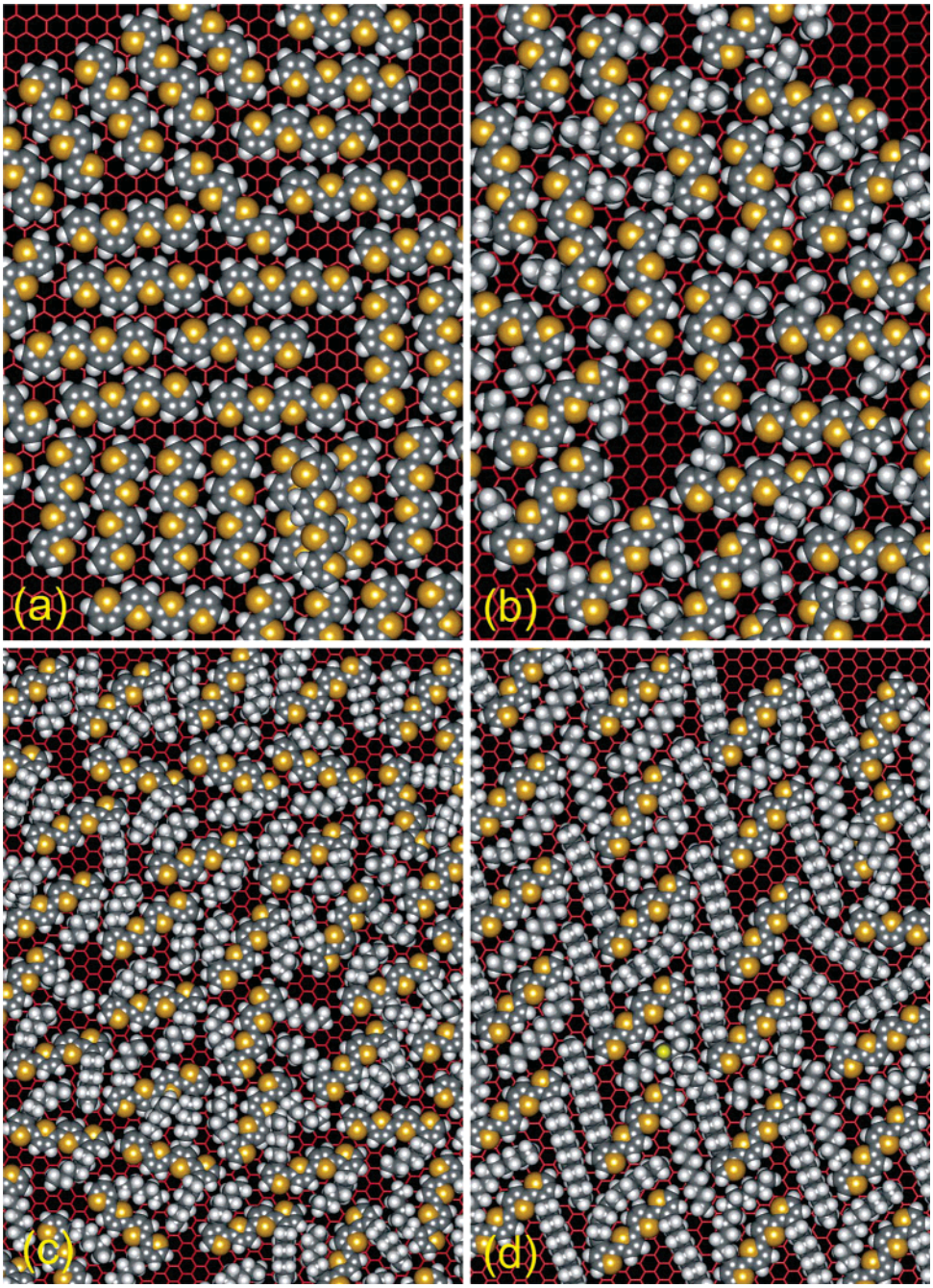

Figure 1. Snapshots from an MD simulation illustrating typical configurations of the molecules adsorbed on a plane of graphite: (a) 4T, (b) 4T3C, (c) 4T6C, and (d) 4T12C. Sulfur atoms are shown in yellow, carbon atoms in dark gray, and hydrogen atoms in light gray. The sizes of all the spheres are space-filling. For visual clarity, the C−C bonds of graphite are depicted as sticks.

observed for the monolayer of closely packed tetrathiophenes is determined by an interplay between van der Waals interactions that tend to stack molecules face-to-face and Coulomb forces that tend to repel equivalent atoms with identical charges in adjacent molecules. For the substituted compounds with long alkyl chains, the molecule−substrate attraction dominates, and as a result, a more planar geometry is preferable. In addition, in the monolayer of such molecules, the distance between conjugated backbones is larger than that for unsubstituted oligomers, so that the intermolecular attraction (per atom) is weaker.

The distribution function $W(\omega_c)$ calculated for substituted oligomers is presented in Figure 3b. It is clear that the orientation of alkyl chains depends on the orientation of thiophene rings. As seen, all the $W(\omega_c)$ functions have a maximum near 10°. Therefore, the hydrocarbon chains do not strictly align parallel to the energetically favorable graphite lattice. For 4T12C, the distribution significantly broadens as compared to 4T3C and 4T6C. In general, such a behavior is consistent with structure factor calculations[48] and modeling studies[51] that indicate that in the solid-state thiophene-based films, there is a torsional twist about the C−C linkage that anchors the hydrocarbon backbone to the polythiophene main chain. It was shown that this has the effect of tilting the alkyl chains so that they can tilt away from the plane of the conjugated backbone and pack into a secondary structure, which loosely approximates the intrinsic packing of saturated hydrocarbons.[48] In the second model,[52,53] the structure is described as having layers of interdigitated, tilted alkyl chains with a 4.5 Å intrastack perpendicular chain-to-chain spacing and a 4 Å side-chain nearest neighbor spacing.[52] A similar

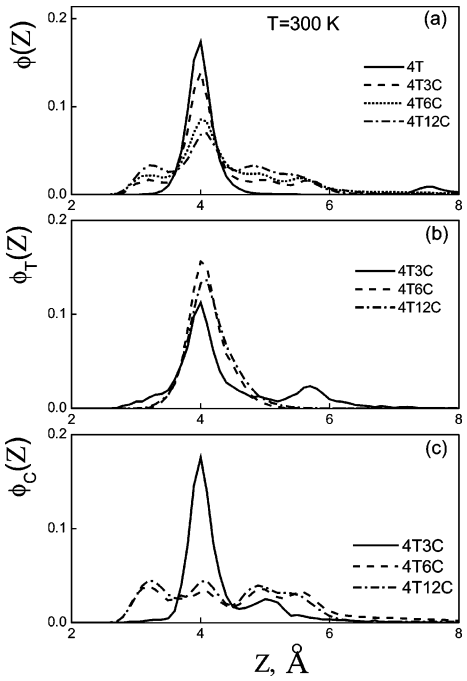

Figure 2. Number−density distribution functions that characterize the sample-average number of atoms at distance z from the graphite surface at $T = 300$ K for (a) all atoms, (b) atoms of the thiophene backbone, and (c) atoms of the alkyl radicals. Note that all the distribution functions are normalized to 1.

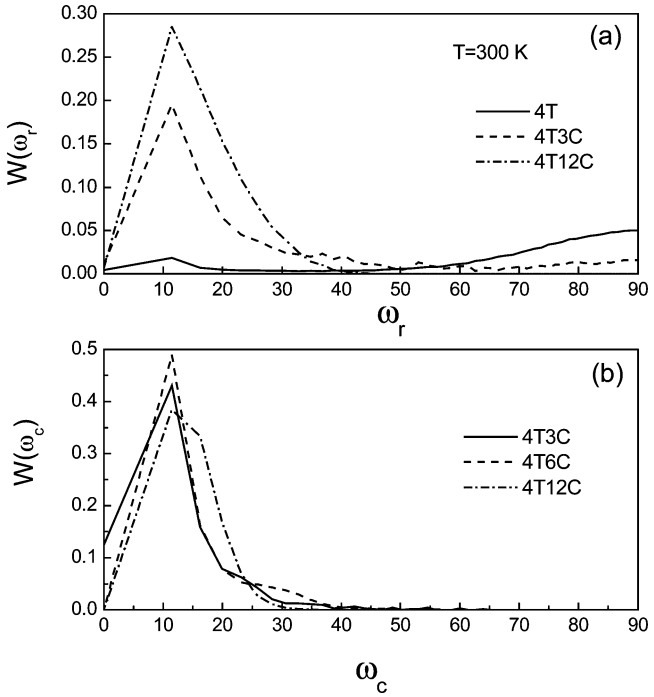

Figure 3. Distribution functions (a) $W(\omega_r)$ for systems 4T, 4T3C, and 4T12C and (b) $W(\omega_c)$ for systems 4T3C, 4T6C, and 4T12C at $T = 300$ K.

structural organization is observed in our simulation (see Figure 1), thereby indicating that both models may be correct for the strongly adsorbed liquid crystalline layers.

As noted in the Introduction, the molecular organization strongly depends on the length of the alkyl substituents.[9−13,16,17] In particular, Azumi et al. imaged a homologue series of oligothiophenes with alkyl substituents in the β-position with STM at the liquid−solid interface.[17] They found that 4Ts bearing sufficiently long (dodecyl and hexyl) side chains exhibited a

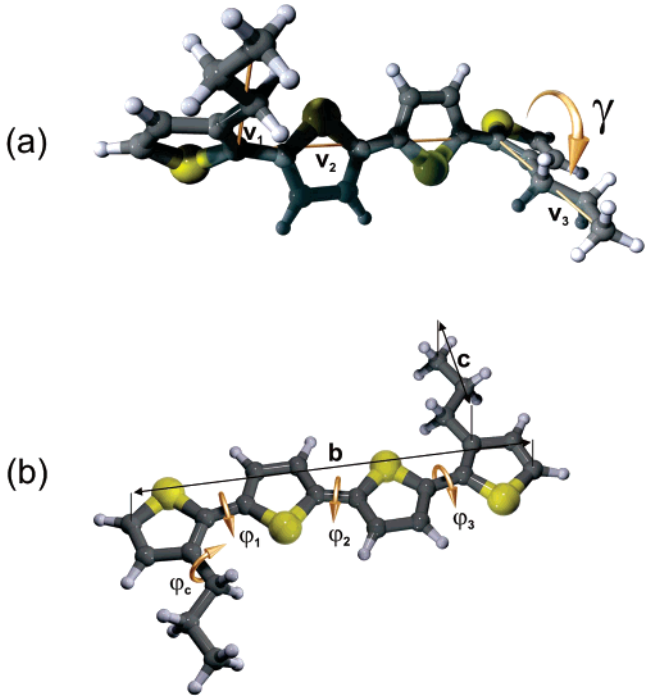

Figure 4. Schemes showing the definition of internal coordinates for a β-substituted tetrathiopene molecule.

nearly planar structure with an interlocking of the hydrocarbon chains on HOPG. On the other hand, the arrangement of propyl-substituted 4T is rather herringbone-like due to the reduced interactions of the shorter side chains with each other and with the substrate. These observations are consistent with those predicted in our simulation.

Molecular Flexibility. The dynamic structure of thiophene-based materials is important to determine physical properties such as thermochromism, in which soft intramolecular motional degrees of freedom are thermally excited.[54,55] These motions are related to twisting/bending-type intramolecular deformations and determined by the existence of the barrier at the planar conformation, or in other words, the competition between the intra- and the intermolecular interaction. It is known that insertion of two alkyl chains on the central thiophene ring creates an important molecular twisting in the polythiophene chain. On the other hand, the length of the thiophene chain as well as the presence of end substituents do not significantly influence the ground-state molecular conformation.[56]

To study the internal flexibility of molecules in the adsorption layer, we introduced an (virtual) intramolecular dihedral angle γ defined by three vectors $\mathbf{v}_1$, $\mathbf{v}_2$, and $\mathbf{v}_3$, as indicated in Figure 4a. The vectors $\mathbf{v}_1$ and $\mathbf{v}_3$ connect the terminal carbon atoms of two hydrocarbon chains with the corresponding carbon atoms on the first and fourth ring. The second quantity characterizing the molecular flexibility is defined by the bending angle γ_c between the plane of a thiophene ring and the virtual bond connecting the terminal chain carbon with the carbon atom of the ring to which the chain is attached.

The distribution functions $W(\gamma)$ and $W(\gamma_c)$, which directly detect the molecular twisting/bending degree of freedom, are shown in Figure 5. The essential features of $W(\gamma)$ are practically the same (irrelevant to the discussion) for 4T3C and 4T6C, but for 4T12C, the simulation predicts a broader population distribution along the twisting angle γ. In particular, the simulation shows an optimal energy structure where the molecular plane defined previously has a dihedral angle of $\gamma = 170°$. Also, there is the second (local) energy minimum at

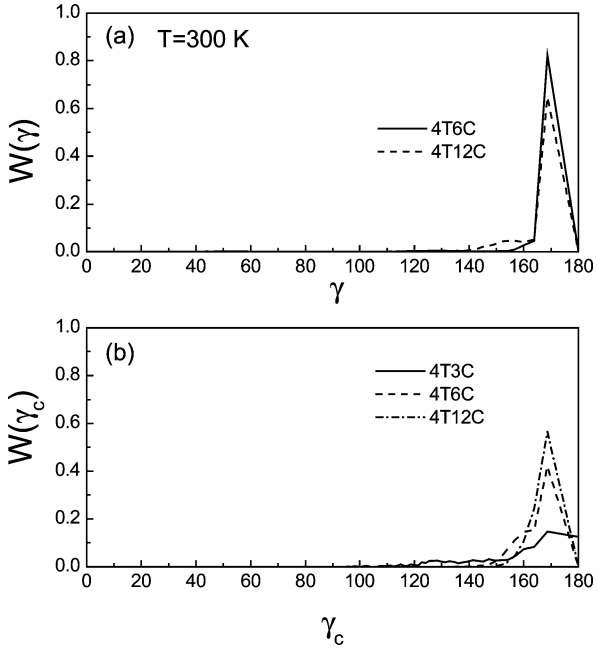

Figure 5. Distribution functions (a) $W(\gamma)$ and (b) $W(\gamma_c)$ characterizing the molecular twisting/bending degree of freedom for the systems 4T3C, 4T6C, and 4T12C at $T = 300$ K.

153° (see Figure 5a). By analyzing the free energy surface, $-k_BT \ln W(\gamma)$, we found that if the molecules have an angle γ close to 180° (coplanarity), those structures are >20 kJ higher in energy. A $\gamma = -10°$ twist of the molecule from 170° costs approximately 7.5 kJ, whereas a −50° twist from 170° costs 12.5 kJ. For 4T3C and 4T6C, those values are 8.2 and ≈21 kJ, respectively, thus demonstrating a larger conformational rigidity of these molecules in the adsorbed layer. In contrast, the molecular deformation related to the motion of alkyl chains needs the lowest (free) energy just for 4T3C, as seen in Figure 5b. Therefore, in this case, the motion of short alkyl radicals is not strongly hindered. The role of this factor will be discussed in more detail next.

Order Parameter. Figure 1 shows that the long axes of the thiophene segment tend clearly to be aligned in rows on the graphite sheet. The molecules do not form a perfect crystalline monolayer but seem to adopt a liquid−crystalline type of order. To compute the order parameter of the molecules, it is necessary to define a molecular axis direction for each molecule. In models that represent the molecules as elongated rigid objects with rotational symmetry about the elongated direction, there is no problem in identifying the axis of a molecule; it is simply the direction of elongation. In fully atomistic MD simulations such as those done here, the molecules are not rigid, and so there is ambiguity in specifiying the direction of each molecule. The method chosen was simply to use the direction of the virtual bond connecting the first and fourth ring in the thiophene backbone as the major direction of the molecule (see Figure 4b). Therefore, the tensor order parameter can be defined by its components through the equation

$$\lambda_{\tau\upsilon} = \frac{1}{2n}\sum_{i=1}^{n}\left[3\frac{b_{i,\tau}b_{i,\upsilon}}{b_i^2} - \delta_{\tau\upsilon}\right] \qquad (2)$$

where n is the number of molecules; $b_{i,\tau}$ and $b_{i,\upsilon}$ are the projections of the vector **b** connecting two outermost carbons (Figure 4b) of the ith molecule on the space fixed axes τ and υ ($\tau, \upsilon = x, y, z$), and $\delta_{\tau\upsilon}$ is the Kronecker delta. The order parameter matrix $||\lambda_{\tau\upsilon}||$ is diagonalizable. Its largest eigenvalue Λ is also referred to as the order parameter, and the eigenvector corresponding to the largest eigenvalue is the director. The Λ function can have a value between 1 indicating parallel alignment and −0.5 indicating perpendicular alignment.

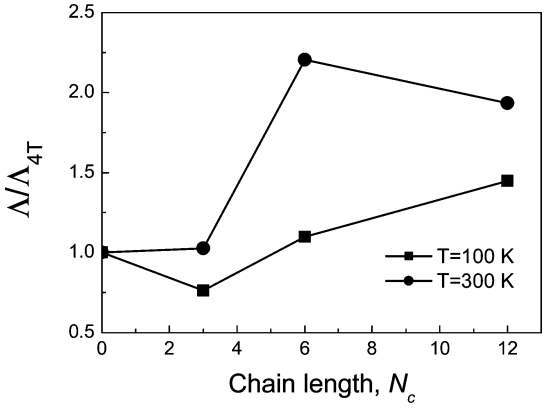

Figure 6. Ratio of the order parameters, Λ/Λ_{4T}, calculated for the vectors **b** (see Figure 4b) as a function of hydrocarbon-chain length, N_c, for two temperatures, 100 and 300 K.

Figure 6 shows the ratio Λ/Λ_{4T} averaged over time and over all molecules as a function of hydrocarbon chain length, N_c, for two temperatures, 100 and 300 K. It is seen that the structure found for substituted oligothiophenes with $N_c > 3$ is more ordered than that predicted for 4T. In general, we observe an increase in the orientational order parameter as the side chains become longer. The effect is more pronounced for higher temperatures. However, the values of Λ calculated at 100 K are larger than those observed at 300 K.

From visual inspection of the large number of snapshots, we concluded that the monolayer composed of unsubstituted tetrathiopenes splits into several subdomains in which the molecules remain aggregated but have three different orientations (see, e.g., Figure 1a). Hence, we observed the coexistence of the three main orientations defined by the atomistic structure of the graphite surface. The nematic order parameter calculated within a subdomain is very high (close to 1), but the Λ value averaged over all the subdomains is rather small (about 0.3 at $T = 300$ K), thus indicating that the system is degenerate with respect to the 120° rotation. For the substituted oligothiophenes with $N_c > 3$, we observed a somewhat different behavior. As is evident, for example, from snapshots shown in Figure 1c,d, although there is a rather high degree of local structural disorder, the molecules, and especially their conjugated backbones, are more or less uniformly oriented in a manner consistent with the nematic liquid crystalline state. We did not observe splitting into subdomains on length scales of the simulated system. As a result, the 2-D orientational order parameter is notably higher.

We also calculated the order parameter for vectors **c**, which defines the orientation of alkyl side chains, as indicated in Figure 4b. The corresponding value of Λ is shown in Figure 7 as a function of temperature, for 4T6C and 4T12C. As expected, the orientational order parameter decreases when the temperature increases. What is relevant here is that its value found for 4T12C is larger than that observed for 4T6C.

Therefore, from the data presented previously, one can conclude that the presence of sufficiently long alkyl substitutes in the β-position facilitates structural ordering in the system of strongly adsorbed oligothiophenes. This clearly indicates that the attachment of side chains to the main conjugated segment changes the interaction between the molecules in the dense layer. That finding is consistent with the experimental results obtained

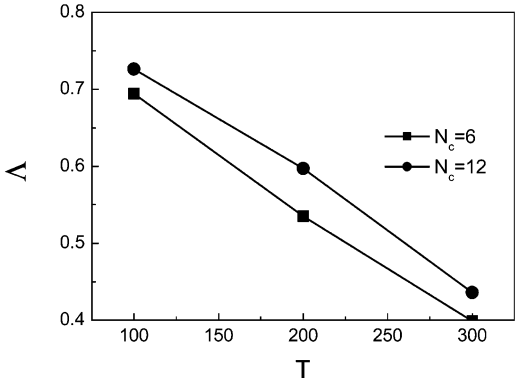

Figure 7. Order parameter defined by the vectors **c** (see Figure 4b) as a function of temperature for the 4T6C and 4T12C systems.

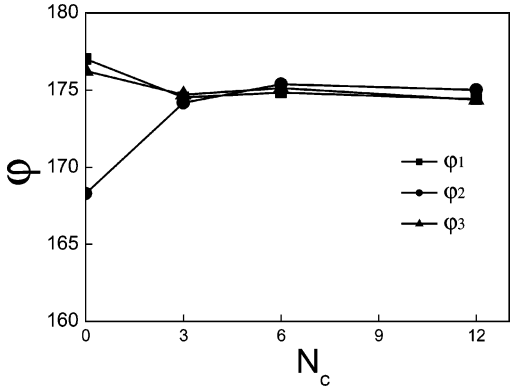

Figure 8. Equilibrium dihedral angles $\varphi_{S-C-C-S}$ (φ_1, φ_2, and φ_3) for three pairs of thiophene rings (see Figure 4b) as a function of hydrocarbon-chain length, N_c, at $T = 300$ K.

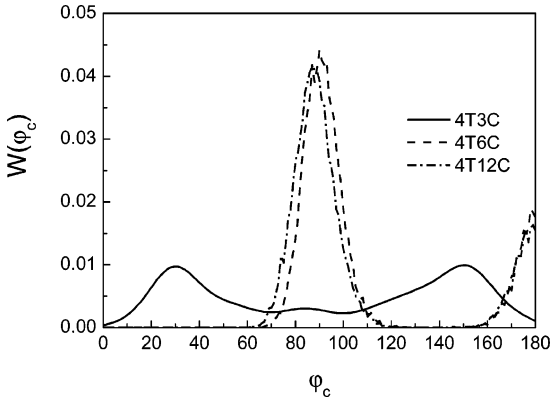

Figure 9. Distribution of side group torsion angles (see Figure 4b) for the three substituted oligothiophenes 4T3C, 4T6C, and 4T12C at $T = 300$ K.

for crystalline surface monolayers.[17] Indeed, it has been found that β-alkylated oligothiophenes with long alkyl side chains form ordered 2-D textures at the highly oriented pyrolitic graphite.[17]

Dihedral Angles. As indicated previously, the orientation of the planes of the aromatic units relative to each other is the most important conformational feature of the molecules. Ab initio gas phase calculations performed on oligothiophenes predict the lowest energy conformations in which the thiophene rings are trans to each other and approximately 30° out of coplanarity.[32] The potential energy surface for twisting the rings from a coplanar conformation to ±30° out of coplanarity is fairly flat, and the structures in this region are within 2−5 kJ of each other, depending on the ab initio method used.[32] Therefore, a fully extended molecular arrangement with dihedral angles between adjacent thiophene rings of $\varphi = 180°$ (trans planar conformation) is possible, especially in the solid-state structure, where packing forces to a great extent determine the equilibrium molecular conformation.[57]

We calculated average dihedral angles $\varphi_{S-C-C-S}$ (φ_1, φ_2, and φ_3) separately for three pairs of thiophene rings (Figure 4b). The equilibrium value of a torsion angle is the result of the interplay between the intrinsic torsion potential at this bond and the repulsive nonbonded interactions and adsorption forces. We found that the torsion angle density distributions for all the backbone torsion angles φ demonstrate only a single sharp peak (not shown). For all the systems, each molecule in the monolayer was found to be nearly planar in an anti (trans) conformation, when the rings have the sulfur atoms pointing alternatively in opposite directions, with the backbone dihedral angles between adjacent thiophene rings mostly distributed in the narrow range of 160−180°. The increase in planarity, as compared to the conformation known for the isolated molecules in the gas phase or in dilute solution ($\varphi \approx 150°$), is due to the packing and adsorption effects occurring in the dense adsorption layer. This is in agreement with the experimental observation that the twist of adjacent rings is about 7° for 4T (see, e.g., ref 58). The average dihedral angles φ_1, φ_2, and φ_3 are shown in Figure 8. Note that the actual value obtained for the angles is somewhat ambiguous, as it has to be determined by sampling and thus depends somewhat on the conditions of the latter. It is seen that the two terminal thiophene rings in 4T lie practically in the same plane (φ_1 and φ_3 are practically the same), while the middle dihedral angle φ_2 demonstrates more significant twisting. For the substituted oligothiophenes, there is no statistically significant difference between the magnitude of φ_1, φ_2, and φ_3, which are close to 180° so that the π-electronic delocalization along a single molecule is expected to be high. However, this indicates that the aromatic rings of adjacent molecules confined as a physisorbed monolayer on a surface are not spatially overlapping and that direct $\pi-\pi$-stacking is not possible.

We also calculated the torsion angle density distribution for the dihedral angle φ_c, which defines the orientation of alkyl side chains (see Figure 4b). Distribution of side group torsion angles for the three substituted oligothiophenes is presented in Figure 9. As seen, the distribution functions found for 4T6C and 4T12C have two peaks near 90 and 180° (trans conformation). In the case of 4T3C, the torsion angle density distribution is very broad, indicating that the propyl radical is more or less freely rotating. This is due to a very low effective barrier separating different conformational states. There is some asymmetry with respect to 90°.

Conclusion

Using atomistic MD simulations, we have investigated the 2-D supramolecular organization of unsubstituted tetrathiopene and β-alkylated oligothiophenes physisorbed on the graphite surface. We have found that the modification of the intramolecular potential by chemical modification of the molecules affects systematically their conformational and adsorption properties, thereby strongly influencing the spatial arrangement of the molecules on the substrate. There are several findings in the simulation that are of considerable interest with respect to the overall picture concerning the supramolecular organization of the strongly adsorbed thiophene derivatives.

The properties of the 2-D phases are considerably affected by the structure of the solid substrate, and its lattice structure can favor the formation of the registered phase.[59] It should be kept in mind that in almost all cases, the gross morphology of

organic monolayer films on graphite can be described as a polycrystalline mosaic with molecules adopting a discrete set of in-plane orientations subject to the constraint of adsorbate−substrate registry, that is, preserving elements of the substrate lattice. This means that the orientational order observed for a macroscopic system should be short-range, extending over distances no greater than a few times the size of the crystalline grains. Therefore, a long-range macroscopic order should be close to zero even if the substrate is a single crystal since normally there is 2-fold or greater rotational symmetry about the surface normal. The presence of the rotational symmetry leads to more than one energetically equivalent molecular orientation (i.e., to the degeneracy of the ground state).[60,61] The situation can be to some extent corrected by reducing the effective molecular symmetry.

The dense monolayer films composed both from unsubstituted and substituted oligothiophenes are commensurate with the graphite substrate. Commensuration is driven primarily through interactions between the substrate and the adsorbed molecules, with the major molecular axis tending to be oriented along one of the three symmetric crystallographic axes in the graphite plane. The combination of the intrinsic symmetry of elongated rod-like unsubstituted tetrathiophenes and the graphite's 3-fold symmetry leads to different but energetically equivalent molecular orientations in the 4T monolayer. In principle, these configurations are observed with equal frequency, and orientational order is only short-range, as discussed previously. On the other hand, when alkyl-substituted oligothiophene molecules adsorb onto graphite, rotation of the long side chains about the C−C bond connecting them to the thiophene ring is strongly hindered (see the data presented in Figure 9 for 4T6C and 4T12C), thereby effectively reducing the molecular symmetry because the adsorption interaction of the thiophene backbone (TB) and the hydrocarbon chains (HC) with the graphite substrate (GS) is different. In other words, for the substituted oligothiophenes adopting a Z-shaped conformation in the strongly adsorbed state, there is a competition between TB−GS and HC−GS interactions, which match the orientation of the molecules in a different way. The hydrocarbon tails and thiophene backbones tend to lay in registry with the substrate, but this is not possible simultaneously for both structural elements. Such competition results in some molecule−substrate incommensurate contact, leading to a decrease in degeneracy and to an increase in the size of orientationally ordered domains and the corresponding order parameter. The effect is clearly demonstrated in Figures 1 and 6. Of course, the surface-induced orientational matching is not the only driving force in shaping the morphology of monolayer films. In fact, it may not even be the most important one for large molecules of complex geometry, when the monolayer structure is dictated by intermolecular packing effects, as in the case of the Z-shaped β-alkylated oligothiophenes. It should also be noted that the potential barriers between adsorption sites are rather shallow, so that even at low temperatures the molecules exhibit a partial mobility resulting in the formation of structural defects.

In the case of the 4T3C monolayer, when the motion of the short alkyl radicals is not strongly hindered (see Figures 5b and 9) and the molecule has an elongated shape, we deal with an intermediate behavior, when the geometrical incompatibility between adsorbent and adsorbate does not play a significant role. It seems that this is one of the reasons for the specific herringbone-like morphology observed for this compound in surface films.[17]

Therefore, chemical modification of the thiophene-based molecules can be an effective method for controlling molecular alignment in monolayer films and their morphology. Certainly, further control of conjugated microstructure in general remains a key issue beyond those of nearest neighbor interactions and simple 2-D packing available in an all-atomic MD simulation.

Acknowledgment. Financial support from SFB-569 (project B13 "Smart Copolymers Near Surfaces") and RFBR is highly appreciated.

References and Notes

(1) *Organic and Biological Optoelectronics*; Rentzepis, P. M., Ed.; University of California, Irvine: Irvine, CA, 1993.
(2) Schopf, G.; Kossmehl, G. *Adv. Polym. Sci.* **1997**, *127*, 1.
(3) *Handbook of Oligo- and Polythiophenes*; Fishou, D., Ed.; Wiley VCh: New York, 1998.
(4) Ohmori, Y.; Uchida, M.; Muro, K.; Yoshino, K. *Jpn. J. Appl. Phys.* **1991**, *30*, 1941.
(5) Roncali, J. *J. Chem. Rev.* **1992**, *92*, 711.
(6) Müller, H.; Petersen, J.; Strohmaier, R.; Gompf, B.; Eisenmenger, W.; Vollmer, M. S.; Effenberger, F. *Adv. Mater.* **1996**, *8*, 733.
(7) Vollmer, M. S.; Effenberger, F.; Stecher, R.; Gompf, B.; Eisenmenger, W. *Chem.—Eur. J.* **1999**, *5*, 96.
(8) Krömer, J.; Rios-Carreras, I.; Fuhrmann, G.; Musch, C.; Wunderlin, M.; Debaerdemaeker, T.; Mena-Osteritz, E.; Bäuerle, P. *Angew. Chem., Int. Ed.* **2000**, *39*, 3481.
(9) Fukunaga, T.; Harada, K.; Takashima, W.; Kaneto, K. *Jpn. J. Appl. Phys.* **1997**, *36*, 4466.
(10) Bäuerle, P.; Fischer, T.; Bidlingmaier, B.; Stabel, A.; Rabe, J. P. *Angew. Chem.* **1995**, *107*, 335.
(11) Bäuerle, P.; Fischer, T.; Bidlingmaier, B.; Stabel, A.; Rabe, J. P. *Angew. Chem., Int. Ed. Engl.* **1995**, *34*, 303.
(12) Azumi, R.; Götz, G.; Bäuerle, P. *Synth. Met.* **1999**, *101*, 569.
(13) Stabel, A.; Rabe, J. P. *Synth. Met.* **1994**, *67*, 47.
(14) Stecher, R.; Gompf, B.; Muenter, J. R. S.; Effenberger, F. *Adv. Mater.* **1999**, *11*, 927.
(15) Stecher, R.; Drewnick, F.; Gompf, B. *Langmuir* **1999**, *15*, 6490.
(16) Azumi, R.; Mena-Osteritz, E.; Boese, R.; Benet-Buchholzd, J.; Bäuerle, P. *J. Mater. Chem.* **2006**, *16*, 728.
(17) Azumi, R.; Götz, G.; Debaerdemaeker, T.; Bäuerle, P. *Chem.—Eur. J.* **2000**, *6*, 735.
(18) Gesquière, A.; Abdel-Mottaleb, M. M. S.; De Feyter, S.; De Schryver, F. C.; Schoonbeek, F.; van Esch, J.; Kellogg, R. M.; Feringa, B. L.; Calderone, A.; Lazzaroni, R.; Brèdas, J. L. *Langmuir* **2000**, *16*, 10385.
(19) De Feyter, S.; Larsson, M.; Gesquière, A.; Verheyen, H.; Louwet, F.; Groenendaal, B.; van Esch, J.; Feringa, B. L.; De Schryver, F. *ChemPhysChem* **2002**, *11*, 966.
(20) Mermin, N. D. *J. Math. Phys.* **1967**, *8*, 1061.
(21) Nelson, D. R.; Halperin, B. I. *Phys. Rev. B* **1979**, *19*, 2457.
(22) Marcon, V.; Raos, G.; Allegra, G. *Macromol. Theory Simul.* **2004**, *13*, 497.
(23) Marcon, V.; Raos, G.; Campione, M.; Sassella, A. *Cryst. Growth Des.* **2006**, *6*, 1826.
(24) Ju, S.-G.; Zeng, Y.-P.; Xing, W.-H. G.; Chen, C.-L. *Langmuir* **2006**, *22*, 8353.
(25) Surin, M.; Leclère, P.; De Feyter, S.; Abdel-Mottaleb, M. M. S.; De Schryver, F. C.; Henze, O.; Feast, W. J.; Lazzaroni, R. *J. Phys. Chem. B* **2006**, *110*, 7898.
(26) Jorgensen, W. L.; Maxwell, D. S.; Tirado-Rives, J. *J. Am. Chem. Soc.* **1996**, *118*, 11225.
(27) Jorgensen, W. L.; McDonald, N. A. *THEOCHEM* **1998**, *424*, 145.
(28) McDonald, N. A.; Jorgensen, W. L. *J. Phys. Chem. B* **1998**, *102*, 8049.
(29) Marcon, V.; Raos, G. *J. Phys. Chem. B* **2004**, *108*, 18053.
(30) Fomine, S.; Guadarrama, P. *J. Phys. Chem. A* **2006**, *110*, 10098.
(31) Salaneck, W. R. *Contemp. Phys.* **1989**, *30*, 403.
(32) Raos, G.; Famulari, A.; Marcon, V. *Chem. Phys. Lett.* **2003**, *379*, 364.
(33) Hernandez, V.; Lopez Navarrete, J. T. *J. Chem. Phys.* **1994**, *101*, 1369.
(34) Tironi, I. G.; Sperb, R.; Smith, P. E.; van Gunsteren, W. F. *J. Chem. Phys.* **1995**, *102*, 5451.
(35) DiCésare, N.; Belletête, M.; Donat-Bouillud, A.; Leclerc, M.; Durocher, G. *Macromolecules* **1998**, *31*, 6289.
(36) McKie, D.; McKie, C. *Essentials of Crystallography*; Blackwell Scientific Publications: Boston, 1986.
(37) Steele, W. A. *Surf. Sci.* **1973**, *36*, 317.
(38) Hentschke, R.; Winkler, R. G. *J. Chem. Phys.* **1993**, *99*, 5528.

(39) Nose, S. *Mol. Phys.* **1986**, *57*, 187.
(40) Hoover, W. G. *Phys. Rev. A* **1985**, *31*, 1695.
(41) Martyna, G. J.; Tobais, D. J.; Klein, M. L. *J. Chem. Phys*. **1994**, *101*, 4177.
(42) Tuckerman, M.; Berne, B. J.; Martyna, G. J. *J. Chem. Phys.* **1992**, *97*, 1990.
(43) Allen, M. P.; Tildesley, D. J. *Computer Simulation of Liquids*; Claredon: Oxford, 1987.
(44) Verlet, L. *Phys. Rev.* **1967**, *159*, 98.
(45) Khalatur, P. G.; Novikov, V. V.; Khokhlov, A. R. *Phys. Rev. E* **2003**, *67*, 51901.
(46) Mologin, D. A.; Khalatur, P. G.; Khokhlov, A. R.; Reineker, P. *New J. Phys.* **2004**, *6*, 133.
(47) Brédas, J. L.; Wudl, F.; Heeger, A. J. *Solid State Commun.* **1987**, *63*, 577.
(48) Prosa, T. J.; Winokur, M. J.; Moulton, J.; Smith, P.; Heeger, A. J. *Macromolecules* **1992**, *25*, 4364.
(49) Bunz, U. H. F. *Chem. Rev.* **2000**, *100*, 1605.
(50) Curtis, M. D.; Cao, J.; Kampt, J. W. *J. Am. Chem. Soc.* **2004**, *126*, 4318.
(51) Xie, X.; O'Dwyer, S.; Corish, J.; Morton-Blake, D. A. *Synth. Met.* **2001**, *122*, 287.
(52) Prosa, T. J.; Winokur, M .J.; McCullough, R. D. *Macromolecules* **1996**, *29*, 3654.
(53) Mena-Osteritz, E.; Meyer, A.; Langeveld-Voss, B. M. V.; Janssen, R. A. E.; Meijer, E. W.; Bäuerle, P. *Angew. Chem., Int. Ed.* **2000**, *39*, 2680.
(54) Ingänas, O.; Salaneck, W. R.; Oästerholm, J. E.; Laakso, J. *Synth. Met*. **1988**, *22*, 395.
(55) DiCésare, N.; Belletête, M.; Donat-Bouillud, A.; Leclerc, M.; Durocher, G. *J. Lumin.* **1999**, *81*, 111.
(56) Riga, J.; Pireaux, J.; Boutique, J.; Caudano, R.; Verbist, J. *Synth. Met.* **1981**, *4*, 99.
(57) De Betten-Dias, A.; Viswanathan, S.; Ruddy, K. *Cryst. Growth Des.* **2005**, *5*, 1477.
(58) van Bolhuis, F.; Wynberg, H. *Synth. Met*. **1989**, *30*, 381.
(59) Dash, J. G. *Films on Solid Surfaces*; Academic Press: New York, 1975.
(60) Somorjai, G. *Introduction to Surface Chemistry and Catalysis*; John Wiley: New York, 1994.
(61) Jensen, P.; Bardotti, L. T.; Barrat, J. L.; Combe, N.; Dupuis, V.; Jamet, M.; Mélinon, P.; Prével, B.; Tuaillon-Combes, J.; Perez, A. In *Nanoclusters and Nanocrystals*; Nalwa, H. S., Ed.; American Scientific Publishers: Valencia, CA, 2003.